Charge-state-dependent energy loss of slow ions. I. Experimental results on the transmission of highly charged ions

Richard A. Wilhelm,[1,*] Elisabeth Gruber,[2] Valerie Smejkal,[2] Stefan Facsko,[1] and Friedrich Aumayr[2]

[1]*Helmholtz-Zentrum Dresden-Rossendorf, Institute of Ion Beam Physics and Materials Research, 01328 Dresden, Germany*
[2]*TU Wien, Institute of Applied Physics, 1040 Vienna, Austria*

We report on energy loss measurements of slow ($v \ll v_0$), highly charged ($Q > 10$) ions upon transmission through a 1-nm-thick carbon nanomembrane. We emphasize here the scaling of the energy loss with the velocity and charge exchange or loss. We show that a weak linear velocity dependence exists, whereas charge exchange dominates the kinetic energy loss, especially in the case of a large charge capture. A universal scaling of the energy loss with the charge exchange and velocity is found and discussed in this paper. A model for charge-state-dependent energy loss for slow ions is presented in paper II in this series [R. A. Wilhelm and W. Möller, Phys. Rev. A **93**, 052709 (2016)].

I. INTRODUCTION

How ions dissipate their energy when moving through matter has been of interest since the early years of the last century [1]. Ions impacting on a solid surface may lose kinetic energy (or, in the case of highly charged ions, also potential energy) as a result of collisions with target electrons and nuclei [2–6]. A corresponding distinction of electronic and nuclear energy loss (so-called "stopping") is usually made but not necessarily justified, since the individual processes involved might be coupled [5,6]. First-order perturbation approaches predict a dependence of the energy loss on the square of the projectile's nuclear charge Z_1 but are only valid at sufficiently high projectile velocities v. Such approaches are, however, inadequate for a heavy ion at low impact velocities [7], where charge exchange, excitation, and ionization processes (involving electrons from the target but also from the projectile) alter the ion's charge state until a dynamic charge- and excitation-state equilibrium of the projectile is reached [8, and references therein] [9–13]. Of course the screening of the Coulomb potential of the nuclear charge by the captured electrons affects the stopping force. This is sometimes taken into account by using an effective charge, a concept that has been pointed out to be somewhat misleading [7] and, at most, empirically justified.

Of interest in this connection is the charge-state dependence of energy loss and, in particular, pre-equilibrium effects, e.g., the energy loss of projectile ions, which have not yet reached their equilibrium charge state. At velocities $v < v_0$ (with v_0 being the Bohr velocity) the equilibrium charge is typically very small ($Q_{eq} \approx Z^{1/3} v/v_0 \leqslant 2$ [14]). Pre-equilibrum phenomena are therefore best studied with slow highly charged ions, whose charge state is far from equilibrium ($10 \leqslant Q \leqslant Z_1$). Since corresponding equilibration lengths in solids are quite small (at most a few nanometers [9,11,15,16]), ultrathin target films are desirable to minimize the projectiles' trajectory in the solid. Information on the equilibration and energy loss dynamics can be important for applications, e.g., nanostructuring of surfaces by slow highly charged ions, since it allows us to estimate the

depth below the surface where the projectiles' potential energy can still be deposited [17–19].

This paper (part I in this series of two papers) presents experimental results on the energy loss (stopping) of slow ($v \ll v_0$), highly charged Xe ions transmitted through a 1-nm thin carbon nanomembrane. We discuss the dependence of energy loss on the incident and exit charge state as well as the impact velocity and present an empirical scaling consolidating our findings. In part II in this series [20] a model for a charge-state-dependent energy loss of slow ions is elaborated and compared with the experimental data regarding charge-state dependence only.

II. EXPERIMENTAL SETUP

Highly charged ions are produced in a room-temperature electron-beam ion trap (EBIT) from Dreebit GmbH, Germany. The base pressure in the ion source is 10^{-10} mbar and during operation a pressure of 3×10^{-9} mbar is maintained by introducing isotopically pure ^{129}Xe gas. A dc ion current is extracted in the leaky mode of the EBIT at a kinetic energy of $4.4\,\text{keV} \times Q$ (Q denotes the ion charge state). An analyzing magnet is utilized to charge state separate the extracted ion beam, which is then focused into a target chamber by several electrostatic lens assemblies. The ion source and beamline are negatively biased with respect to the target chamber, which allows us to decelerate the ion beam when it enters the target chamber at ground potential. (The ion source is additionally biased at $+4.4$ kV with respect to the beamline.) A final electrostatic lens assembly, the deceleration lens, reaches into the chamber to reduce the field free flight pass as much as possible. Even at the lowest (final) kinetic energy, 4 keV, a beam spot size of around 1 mm in diameter can be maintained. The target chamber is kept under ultrahigh vacuum conditions (10^{-9} mbar) during measurements. An electrostatic analyzer with a relative energy resolution of $\Delta E/E \approx 1.5 \times 10^{-3}$ is mounted in the target chamber and allows energy- and charge-state separation of the ions after transmission through thin samples. The analyzer can be rotated around the sample axis in order to perform angle-resolved transmission measurements.
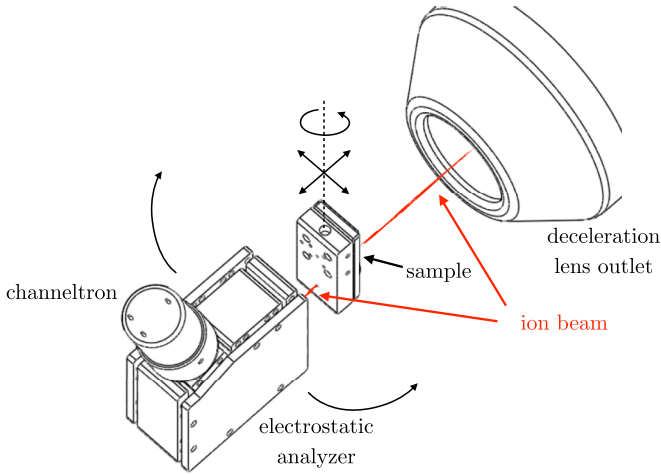
---
*r.wilhelm@hzdr.de

FIG. 1. Sketch of the ion beam passing through the sample holder into the electrostatic analyzer. The analyzer can be rotated around the sample.

Ions are counted in a Hamamatsu Photonics channeltron after passing through the analyzer.

Figure 1 shows a sketch of the sample-analyzer arrangement in the chamber with the respective axes of movement for the sample and analyzer.

Samples are produced by CNM Technologies Bielefeld, Germany, by cross-linking a self-assembled monolayer of biphenyl-4-thiol molecules on a Au substrate with low-energy electrons [21]. The cross-linked monolayer is released from the substrate by chemical etching and transferred to a standard transmission electron microscopy (TEM) grid with a thick lacey-carbon support. A load lock is used to bring the TEM grid into the target chamber without breaking the vacuum in the chamber or beamline.

Before the actual transmission experiments, the energy- and charge-state distributions of the ion beam were checked without samples. The incident kinetic energy E_0 has a width of $\Delta E_0 \approx 10^{-3} E_0$ and is thus smaller than the measurement resolution. A small charge exchange with $Q \rightarrow Q - 1$ of the order of 10^{-3} was observed due to scattering with rest gas atoms in the approximately 5-m-long beamline. Since the charge exchange discussed here is 1 to 2 orders of magnitude more intense, combined with a much larger ΔQ, we regard the incoming beam as being prepared exclusively in the desired charge state Q.

III. MEASUREMENTS

The ion transmission of highly charged xenon through the described carbon nanomembranes results in a spectrum of exit charge states. The spectrum is twofold as depicted in Fig. 2 and discussed in [22].

The energy loss, however, is dependent on the exit charge state Q_{exit} (or, in other words, on the charge exchange $\Delta Q = Q_{in} - Q_{exit}$). Additionally, electronic stopping is considered to scale linearly with the ion velocity for slow ions [4,23]. We measured the velocity dependence of the energy loss and the results are shown in Fig. 3 for Xe^{20+} ions. The energy loss increases with the velocity between 1.5×10^5 and 2.5×10^5 m/s
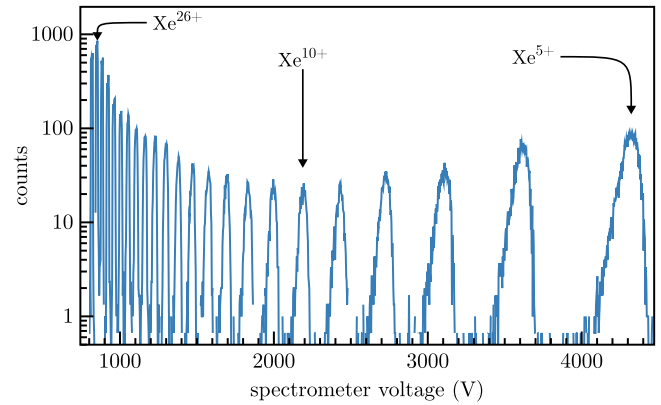

FIG. 2. Exit charge-state spectrum of Xe^{28+} ions at $E_{\mathrm{kin}} = 126$ keV transmitted through a 1-nm-thick carbon nanomembrane. The spectrum is bimodal.

for the lower exit charge states ($Q_{\mathrm{exit}} \leqslant 5$). For higher exit charge states, i.e., smaller charge exchanges, the dependence on the ion velocity gets smaller and almost vanishes. At the even higher velocity of 3.6×10^5 m/s the energy loss decreases, thus the linear velocity scaling is not preserved in case of highly charged ions [24]. Figure 3 already shows that the energy loss depends on more than one parameter in a complex way.

Figure 4 shows the energy loss as a function of the exit charge state Q_{exit} or charge loss $\Delta Q = Q_{\mathrm{in}} - Q_{\mathrm{exit}}$ for different ion velocities, ranging from 1.8×10^5 m/s ($0.08v_0$) to 3.7×10^5 m/s ($0.17v_0$). Here a common dependence on the charge exchange can already be seen.

The energy loss is strongly dependent on the charge exchange, but also on the incident charge state and/or velocity. However, the velocity dependence is small.

A quadratic dependence of the energy loss on the incident charge state is commonly assumed in the literature [25] and was recently measured in experiments [22]. Figure 5 shows
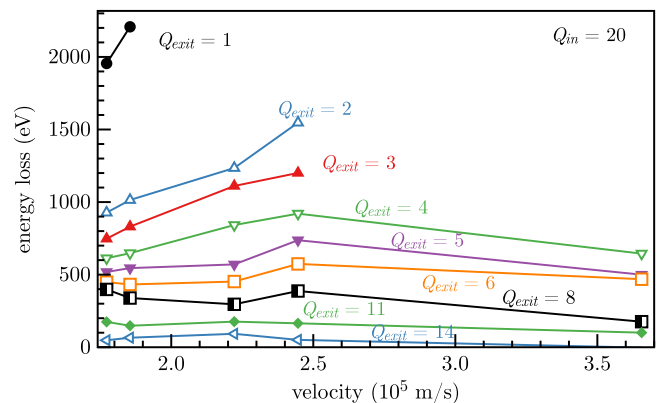

FIG. 3. Energy loss of Xe^{20+} transmitted through a 1-nm-thick carbon nanomembrane as a function of the ion velocity for different observed charge exchanges (exit charge states). For a large charge exchange and a velocity around 2×10^5 m/s the energy loss increases with the velocity, whereas it becomes independent of the velocity for a smaller charge exchange. For a higher velocity, about 3.6×10^5 m/s, the energy loss decreases.
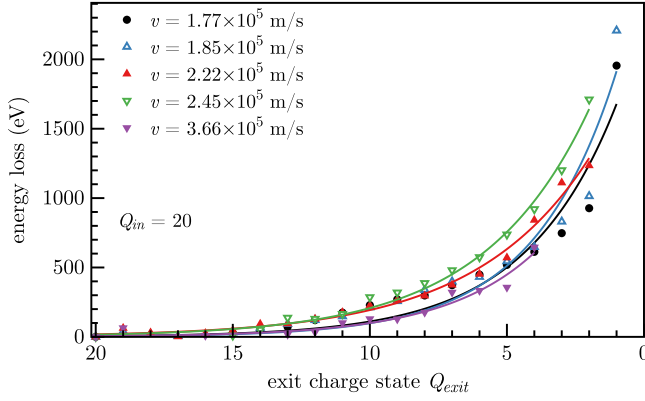
FIG. 4. Energy loss as a function of exit charge state for different ion velocities v and $Q_{\text{in}} = 20$. The target material is again a 1-nm-thick carbon nanomembrane. The data are fitted by a function $\alpha e^{\beta(Q_{\text{in}} - Q_{\text{exit}})/Q_{\text{in}}}$ (see text).

the incident charge-state dependence of the energy loss for a fixed ion velocity and different exit charge states (charge exchange). Here, the quadratic dependence can be seen as well (dotted-dashed line for $Q_{\text{exit}} = 2$). The data points are also fitted with the function $\Delta E = \alpha + \beta Q_{\text{in}} e^{\gamma(Q_{\text{in}} - Q_{\text{exit}})/Q_{\text{in}}}$, which results from a universal scaling of our results with the charge exchange (see below). The quadratic fit and the universal scaling fit the data in Fig. 5 equally well. Thus, we cannot unambiguously distinguish between a quadratic dependence and an exponential dependence on Q_{in} here, whereas only the latter fits the data in Figs. 4, 5, and 6 simultaneously. The parameters α, β, and γ range from 50 to 240 eV, 2×10^{-4} to 0.5 eV, and 8 to 14, respectively. Note that the exponent ranges only from 0 to γ ($\Delta Q / Q_{\text{in}} \leqslant 1$).

Summarizing, we see a weak dependence of the energy loss on the ion velocity (Fig. 3), a strong dependence on charge loss or exchange (Fig. 4), and a quadratic dependence on the incident charge state (Fig. 5).
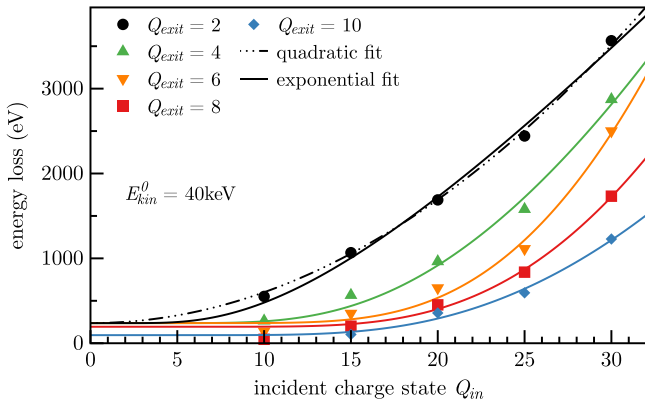

FIG. 5. Energy loss of Xe ions transmitted through a 1-nm-thick carbon nanomembrane as a function of the incident charge state for different charge exchanges (exit charge states). The primary kinetic energy is fixed to 40 keV. All energy loss data were fitted with the function $\Delta E = \alpha + \beta Q_{\text{in}} e^{\gamma(Q_{\text{in}} - Q_{\text{exit}})/Q_{\text{in}}}$ (see text). To compare with the $Q_{\text{exit}} = 2$ data, a quadratic fit is shown as suggested recently in [22].
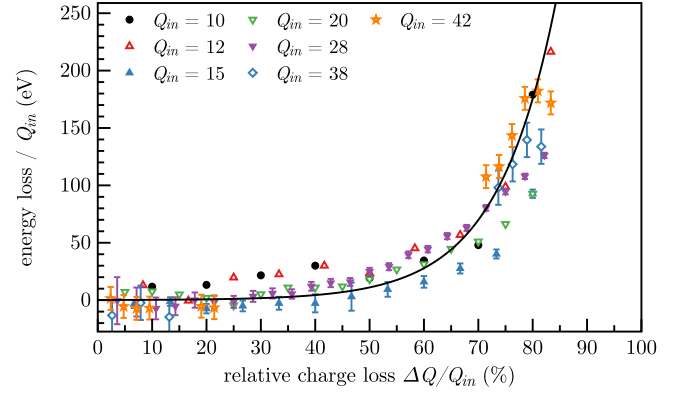

FIG. 6. Energy loss as a function of relative charge loss $\Delta Q / Q_{\text{in}}$ for different incident charge states of Xe and also different incident kinetic energies of $E_{\text{kin}} = 4400$ eV $\times Q_{\text{in}}$. The energy loss was rescaled by a factor Q_{in}^{-1} (see text), whereas now all energy losses follow a single-exponential function. Negative values are a result of the limited measurement accuracy.

To find a universal scaling of the energy loss, ions at different incident charge states from $Q_{\text{in}} = 10$ to $Q_{\text{in}} = 42$ were used at different kinetic energies of 4400 eV $\times Q_{\text{in}}$ (44 to 185 keV), i.e., different ion velocities. The energy loss was measured for each exit charge state, thus all three parameters are varied now. The data are shown in Fig. 6, where the measured energy loss is rescaled by a factor Q_{in}^{-1}. In fact, the rescaled energy losses all follow the same dependence on the (relative) charge exchange $\Delta Q / Q_{\text{in}}$. The fit function is again the same as in Figs. 4 and 5, i.e., $\Delta E / Q_{\text{in}} = \beta e^{\gamma \Delta Q / Q_{\text{in}}}$, with $\beta = 0.11$ eV and $\gamma = 9.2$. At this point we cannot explain the universal scaling due to the lack of a charge-exchange-dependent energy loss model but, rather, see this as an empirical finding stimulating future theoretical work.

IV. SUMMARY AND CONCLUSION

The electronic energy loss ΔE at low velocities is considered to be proportional to the ion velocity v,

$$\Delta E(v, Q_{\text{in}} \approx 0) \propto v, \qquad (1)$$

which was not confirmed in our measurements. Note that the data presented here were acquired under a normal exit angle ($0°$), where nuclear losses are only of minor importance. For larger scattering angles (up to $5°$) nuclear losses and their velocity dependence should be considered. However, we see a strong dependence on the incident and exit charge states,

$$\Delta E(v, Q_{\text{in}}, Q_{\text{exit}}) \propto f(Q_{\text{in}}, Q_{\text{exit}}), \qquad (2)$$

where $f(Q_{\text{in}}, Q_{\text{exit}})$ must be determined. In order to find $f(Q_{\text{in}}, Q_{\text{exit}})$ we showed that

$$\Delta E(v = \text{const}, Q_{\text{in}}, Q_{\text{exit}}) \propto \delta(Q_{\text{exit}}) Q_{\text{in}}^2 \quad \text{or} \qquad (3)$$

$$\propto Q_{\text{in}} e^{\gamma \frac{Q_{\text{in}} - Q_{\text{exit}}}{Q_{\text{in}}}} \qquad (4)$$

(β and γ are constants, and δ is some function depending on Q_{exit}) and

$$\Delta E(v, \Delta Q / Q_{\text{in}}) \propto Q_{\text{in}} e^{\gamma \frac{\Delta Q}{Q_{\text{in}}}}. \qquad (5)$$

The velocity dependence is weak and the energy loss is dominated by charge exchange. The exponential dependence on charge exchange is found by comparing different data sets (see Fig. 6) and finding a common fit function. Note that Eq. (3) can easily be obtained from Eq. (4) by a simple Taylor expansion. The universal form, (5), contains implicitly the velocity dependence, because the energies used are 4400 eV $\times Q_{in}$ and thus the velocities scale with $\sqrt{Q_{in}}$.

Additionally to the explicit velocity dependence discussed here, charge exchange may also depend on the ion velocity (i.e., $\Delta Q = \Delta Q(v)$). Charge exchange from resonant charge transfer $\Delta Q_{res}(v)$ depends strongly on the velocity, because it determines the time frame for charge transfer. Nonetheless, resonant charge transfer does not contribute to energy loss [26]. Nonresonant charge transfer ΔQ_{nonres} as in the case of close ion-target approach and quasimolecule formation [27,28], on the other hand, may contribute to energy loss, whereas it does not depend on the ion velocity (in the velocity range discussed here). The bimodal exit charge-state distribution in our measurements for carbon nanomembranes was attributed to different impact parameter regimes upon collisions from the angular dependence of the charge exchange [22]. A small charge exchange, associated with large target-projectile distances, may therefore only result from resonant charge transfer, i.e., here $\Delta Q = \Delta Q_{res}(v) \ll Q_{in}$. A large charge exchange, on the contrary, contains contributions from both resonant and nonresonant charge transfer, i.e., $\Delta Q = \Delta Q_{res}(v) + \Delta Q_{nonres} \lesssim Q_{in}$.

---

[1] N. Bohr, Philos. Mag. **25**, 10 (1913).

[2] H. Bethe, Ann. Phys. **397**, 325 (1930).

[3] F. Bloch, Ann. Phys. **408**, 285 (1933).

[4] J. Lindhard and M. Scharff, Phys. Rev. **124**, 128 (1961).

[5] P. Sigmund, Phys. Rev. A **54**, 3113 (1996).

[6] P. Sigmund, Phys. Rev. A **56**, 3781 (1997).

[7] P. Sigmund, Mat. Meddelelser Udgivet Af Det K. Danske Vidensk. Selsk. **52**, 557 (2006).

[8] H.-D. Betz, Rev. Mod. Phys. **44**, 465 (1972).

[9] R. Herrmann, C. L. Cocke, J. Ullrich, S. Hagmann, M. Stäckli, and H. Schmidt-Böcking, Phys. Rev. A **50**, 1435 (1994).

[10] S. Winecki, C. L. Cocke, D. Fry, and M. P. Stöckli, Phys. Rev. A **53**, 4228 (1996).

[11] M. Hattass, T. Schenkel, A. V. Hamza, A. V. Barnes, M. W. Newman, J. W. McDonald, T. R. Niedermayr, G. A. Machicoane, and D. H. Schneider, Phys. Rev. Lett. **82**, 4795 (1999).

[12] M. Imai, M. Sataka, K. Kawatsura, K. Takahiro, K. Komaki, H. Shibata, H. Sugai, and K. Nishio, Nucl. Instrum. Methods Phys. Res. Sec. B **267**, 2675 (2009).

[13] E. Lamour, P. D. Fainstein, M. Galassi, C. Prigent, C. A. Ramirez, R. D. Rivarola, J.-P. Rozet, M. Trassinelli, and D. Vernhet, J. Phys.: Conf. Ser. **635**, 032022 (2015).

[14] N. Bohr, Mat. Meddelelser Udgivet Af Det K. Danske Vidensk. Selsk. **18**, 1 (1948).

[15] T. Schenkel, M. A. Briere, A. V. Barnes, A. V. Hamza, K. Bethge, H. Schmidt-Böcking, and D. H. Schneider, Phys. Rev. Lett. **79**, 2030 (1997).

[16] F. Allegrini, R. W. Ebert, S. A. Fuselier, G. Nicolaou, P. Bedworth, S. Sinton, and K. J. Trattner, Opt. Eng. **53**, 024101 (2014).

[17] A. El-Said, R. Neumann, K. Schwartz, and C. Trautmann, Nucl. Instrum. Methods Phys. Res. Sec. B **245**, 250 (2006).

[18] C. Lemell, A. El-Said, W. Meissl, I. Gebeshuber, C. Trautmann, M. Toulemonde, J. Burgdörfer, and F. Aumayr, Solid State Electron. **51**, 1398 (2007).

[19] A. S. El-Said, R. Heller, W. Meissl, R. Ritter, S. Facsko, C. Lemell, B. Solleder, I. C. Gebeshuber, G. Betz, M. Toulemonde, W. Möller, J. Burgdörfer, and F. Aumayr, Phys. Rev. Lett. **100**, 237601 (2008).

[20] R. A. Wilhelm and W. Möller, Phys. Rev. A **93**, 052709 (2016).

[21] A. Turchanin and A. Gölzhäuser, Prog. Surf. Sci. **87**, 108 (2012).

[22] R. A. Wilhelm, E. Gruber, R. Ritter, R. Heller, S. Facsko, and F. Aumayr, Phys. Rev. Lett. **112**, 153201 (2014).

[23] O. B. Firsov, Sov. Phys. JETP **36**, 1076 (1959).

[24] F. F. Komarov and M. A. Kumakhov, Phys. Status Solidi **58**, 389 (1973).

[25] J. F. Ziegler, J. P. Biersack, and U. Littmark, *The Stopping and Range of Ions in Solids (Vol. 1. Stopping and Range of Ions in Solids)*, edited by J. Ziegler (Pergamon Press, New York, 1985).

[26] J. I. Juaristi, A. Arnau, P. M. Echenique, C. Auth, and H. Winter, Phys. Rev. Lett. **82**, 1048 (1999).

[27] N. Stolterfoht, A. Arnau, M. Grether, R. Köhrbrück, A. Spieler, R. Page, A. Saal, J. Thomaschewski, and J. Bleck-Neuhaus, Phys. Rev. A **52**, 445 (1995).

[28] A. Arnau, R. Köhrbrück, M. Grether, A. Spieler, and N. Stolterfoht, Phys. Rev. A **51**, R3399 (1995).